



Effect of RE addition on solidification process and high-temperature strength of Al–12%Si–4%Cu–1.6%Mn heat-resistant alloy

Heng-cheng LIAO, He-ting XU, Yi-yun HU

Jiangsu Key Laboratory for Advanced Metallic Materials,
School of Materials Science and Engineering, Southeast University, Nanjing 211189, China

Received 28 August 2018; accepted 7 March 2019

Abstract: The effect of RE addition on solidification process and high-temperature strength of Al–12%Si–4%Cu–1.6%Mn (in wt.%) heat-resistant alloy was investigated by microstructure observation and tensile test. A great number of fine needle-like RE-rich phases are observed in the alloys with RE addition. Solutionizing treatment does not change their morphologies and sizes, indicating that they have good thermal stability. The addition of RE totally alters the solidification process of eutectic CuAl₂ phase, from network-like phase in the form of segregation at the final eutectic grain boundaries to discretely blocky phase growing on the hair-filamentous RE-rich needles. In the alloys with Ce addition, blocky CuAl₂, particulate Al₁₅Mn₃Si₂ and needle-like RE-rich needle phases grow together, but they did not occur in the alloy with only La addition. The addition of RE does not considerably improve the strength of the alloy at high temperatures. The formation of RE-rich phases also does not significantly alter the originating and propagating of micro-cracks in the alloy during tensile test.

Key words: Al–Si–Cu–Mn heat-resistant alloy; rare earth; solidification process; high-temperature strength

1 Introduction

The cylinder block and cover are the most important and key components of an engine. Due to their complex shape, casting is actually the sole manufacturing method. High power density engines, such as aluminum diesel engines that are gaining more attention, are required to work at a temperature above 300 °C. The development of heat-resistant casting aluminum alloys offers great challenging opportunities.

Al–Si–Cu–Mg heat-resistant alloys have been widely used to manufacture engines for small passenger cars. Some examples are A380, A319 and ZL702A aluminum alloys [1–3]. In these alloys, CuAl₂ phase acts as the main heat-resistant strengthening phase along with Al₄CuMg₅Si₄ (*W*-phase), Al₅Mg₈Si₆Cu₂ (*Q*-phase) and/or other complex intermetallic compound phases from alloying. Alloying (such as Ni, Cr, Fe, Li) [3–5] and micro-alloying (for example, Ti, Zr, B, Y, Hf, Nb, Ta, Cr and Mo) [6,7] have been used to improve the high-temperature strength of Al–Si–Cu–Mg heat-resistant

alloys. Manganese is an important alloying element in Al–Cu–Mn heat-resistant alloys [8,9]. Manganese addition in Al–Si–Cu alloys, generally with a low content less than 0.5 wt.%, is usually used to neutralize the detrimental effects of β -Al₅FeSi by transforming it to α -Al₁₅(Mn,Fe)₃Si₂ phase [10–12]. LIAO et al [13] developed a novel heat-resistant aluminum alloy by introducing high content of Mn in near-eutectic Al–12%Si–4%Cu (wt.%) alloy, in which the primary and eutectic Al₁₅Mn₃Si₂ phase has much better thermal stability than CuAl₂ phase. Combined addition of Mn and Cr into near-eutectic Al–Si–Cu alloy could significantly alter the morphology of the primary Al₁₅Mn₃Si₂ phase, thus remarkably improving the high-temperature strength, more than 100 MPa at 350 °C [14].

RE elements have been widely used in aluminum alloys, mainly to refine the microstructure and hence to improve the mechanical properties of the alloys at room temperature [15,16]. LI et al [17] investigated the effect of La addition on the high temperature properties of ZL702 alloy. ZHANG et al [7] investigated the influence of Y addition (0.05%, 0.1%, 0.15%, 0.2%, 0.25%, 0.5%

and 0.8%, in wt.%) on mechanical properties at 250 °C and reported that the alloy with 0.1% Y had the highest strength due to the refining effect of trace Y addition on eutectic Si phase. FAN et al [18] reported that the addition of Ce could lead to a morphology change of α -Al₁₅(Fe,Mn)₃Si₂ from coarse Chinese-script into small and discrete block. In 2A14 aluminum alloy with addition of Ce-rich mish-metal, CeAl₄, LaAl₄ and Al₈Cu₄Ce phases were observed at grain boundary [19].

However, the role of RE addition in heat-resistant aluminum alloys was not well investigated, especially on solidification process and high-temperature strength. In this study, the effects of mish-metal, La and Ce on the solidification process and high-temperature strength of the Al–12%Si–4%Cu–1.6%Mn alloy were discussed by microstructure observation, phase structure analysis and tensile test at different temperatures.

2 Experimental

The studied alloys were prepared in a graphite crucible of 3 kg capacity using a melting/vacuum holding furnace with Al–12.5wt.%Si, Al–10wt.%Sr, Al–10wt.%Mn, Al–5wt.%Ce and Al–5wt.%La master alloys, and commercial purity Cu (99.8 wt.%) ingot, Si (98 wt.%) blocky-shaped particles, and Ce-rich misch metal (MM, the mass fraction of La+Ce more than 80%). After processing, the melt was poured at 993 K (720 °C) into a cast iron mold (with a plate-like cavity of 170 mm × 100 mm × 20 mm, preheated at 523 K (250 °C) for 5 h). The final chemical composition of the alloys was analyzed using MAXx LMF15 spark emission spectrometer, as listed in Table 1. However, MM, La and Ce are marked as the addition levels because of no corresponding detection channels. Metallographic samples were cut from the castings, and etched with a mixed acid reagent (20 mL HCl + 20 mL HNO₃ + 5 mL HF + 55 mL H₂O) for 15 s. Microstructural observation was carried out using an OLYMPUS BX60M metallographic microscope and a scanning electron microscope (SEM) equipped with EDS. The X-ray diffraction (XRD, D8-Discover equipped with Cu K_α radiation) was used to analyze phase constituents with $2\theta=10^\circ\text{--}55^\circ$ and a scanning step of 0.02 (°)/step.

Table 1 Compositions of studied alloys (wt.%)

Alloy	Si	Cu	Mn	Sr	RE*
S4	12.31	4.02	1.71	0.0258	0
S4-1	11.94	4.12	1.59	0.0243	0.5 MM
S4-2	11.86	3.84	1.63	0.0263	1.0 MM
S4-3	12.41	4.19	1.60	0.0253	0.5 La
S4-4	12.24	4.09	1.57	0.0262	0.5 Ce

* Addition level

In order to estimate the RE addition effect on high-temperature strength, the castings were firstly solutionized at 510 °C for 5 h and further aged at 165 °C for 6 h [13], and then machined into standard tensile samples (GB6397–86) with a gauge size of 35 mm × 10 mm × 3 mm. High-temperature tensile tests (at 200 and 300 °C) were carried out on a CMT5105 electronic universal testing machine with a rate of 1 mm/min. This provided a strain with the order of 10⁻⁴ s⁻¹. The ultimate tensile strength was taken as an average of 3 replicates.

3 Results and discussion

3.1 Microstructure and solidification process

Figure 1 shows the microstructures of the as-cast alloys with or without RE addition. The addition of RE is expected, to some extent, to afford heterogeneous nucleation sites for the primary Al₁₅Mn₃Si₂ phase in Al–12Si–4Cu–1.6Mn alloy. However, RE addition has almost no influence on the morphology and size of the primary Al₁₅Mn₃Si₂ phase. But, interestingly, there are a large number of fine needles, some are black and curved hair-like, in the microstructure of the alloys with addition of RE, whether sole addition of La and Ce, or combined addition in the form of MM. And the amount is increased with the addition level of RE (Figs. 1(b) and (c)), even full of the whole field of view.

The fine needles are RE-rich phases. Their SEM images and EDS results are shown in Fig. 2. In S4-1 alloy with addition of MM, these needles contain La and Ce. And in S4-2 and S4-3 alloys, the needles are La-rich and Ce-rich, respectively. Fine RE-rich needles are also observed at the grain boundaries of 2A14 aluminum alloy with Ce-rich mish-metal addition [19]. All needles are detected to contain high level of Cu. The RE-rich needles are, somewhere bright and thick, somewhere black and thin. The RE-rich needles in S4-4 alloy, which was etched for 30 s, are re-observed by SEM–EDS, as shown in Fig. 3. These needles do not seem to be cylinder rods but square bars, in form of typical faceted-growth. Of more importance, obviously, these needles are multi-structural, of which the surface is a thin film enveloping the inner. The EDS results illustrate the difference of Cu content at different detected positions. All of the detected EDS results on these needles reveal that they contain La or Ce as well as high levels of Si and Cu. It is well known that the EDS results are very inaccurate for fine phase, because the detected region by EDS ray is much huger than the selected area. From EDS results, it is just surely concluded that these needles contain high level of La or Ce. So, the RE-rich needles may be grey and very fine. When the RE-rich needles are enveloped by CuAl₂ film, they become bright in contrast and thickened in size (typically in Fig. 2).

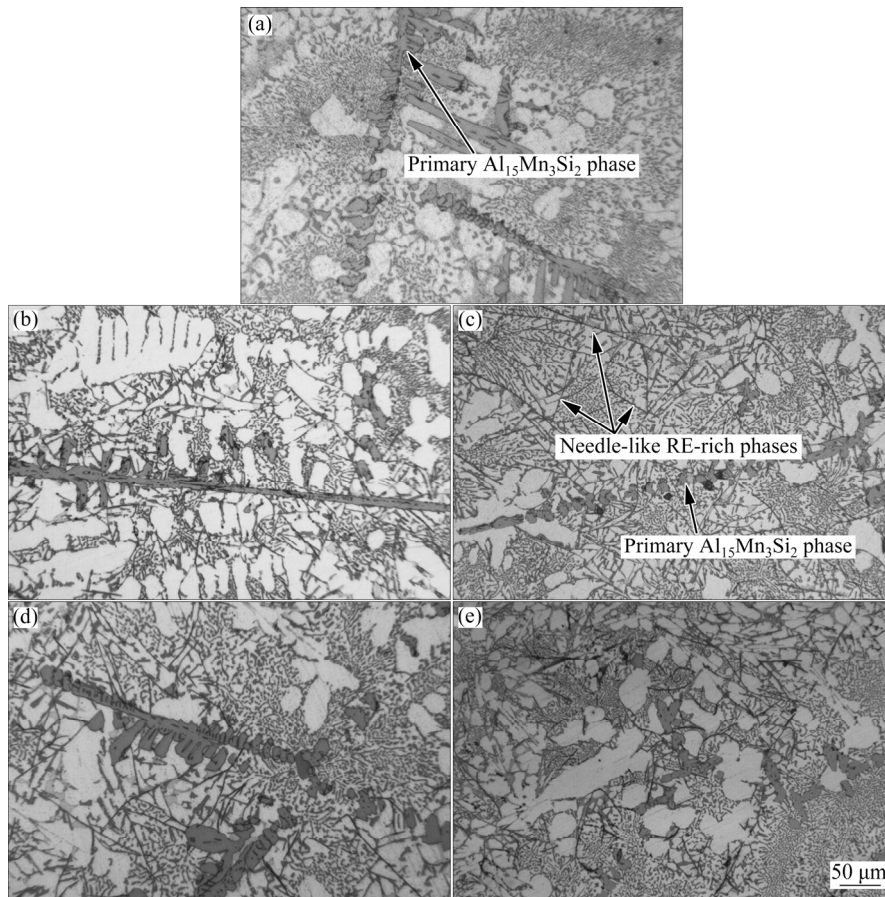


Fig. 1 Optical microscopic images showing microstructures of as-cast alloys with different RE additions: (a) S4 alloy; (b) S4-1 alloy; (c) S4-2 alloy; (d) S4-3 alloy; (e) S4-4 alloy

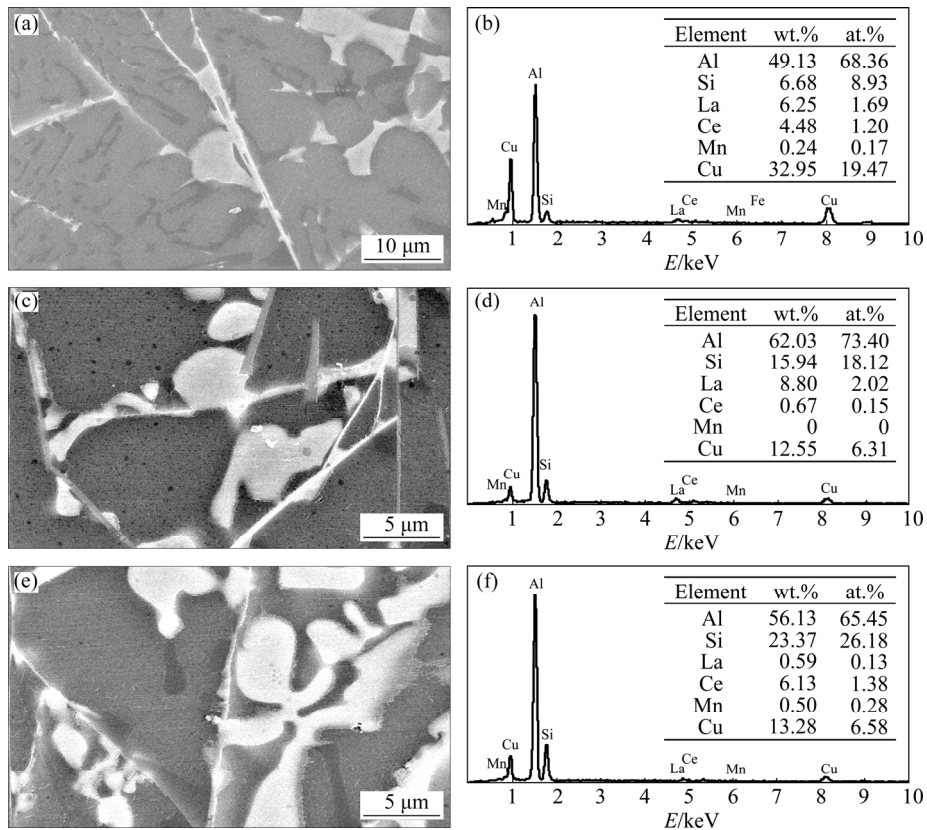


Fig. 2 SEM images (a, c, e) and their EDS results (b, d, f) of RE-rich phases in S4-1(a, b), S4-3(c, d) and S4-4 (e, f) alloys

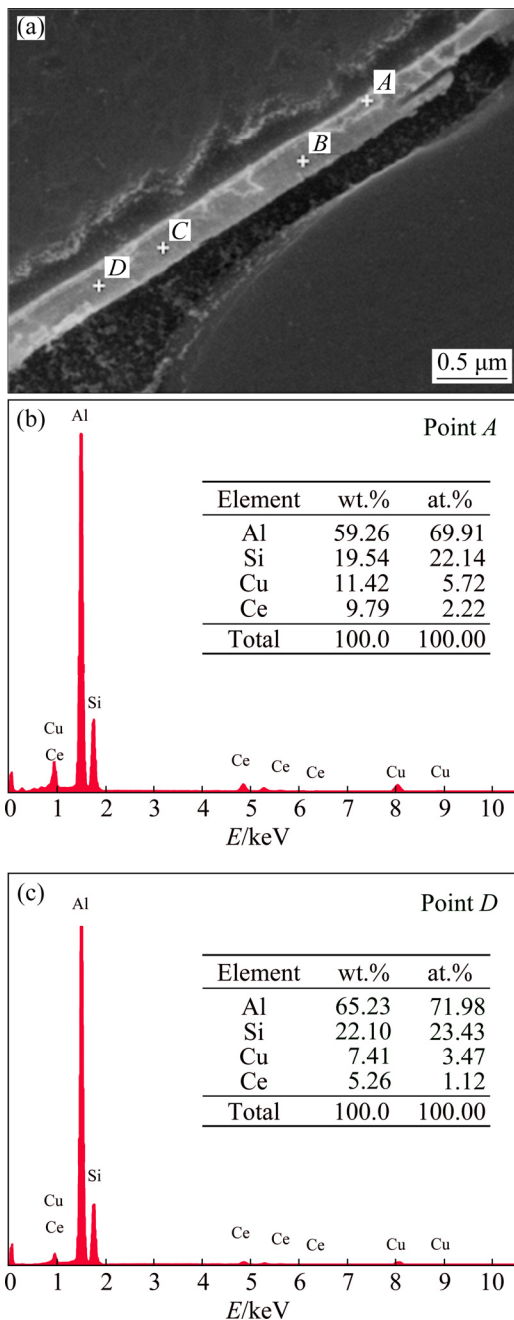


Fig. 3 SEM image (a) and EDS results at different positions (b, c) of needle-like phases in S4-4 alloy etched for 30 s

Figures 4(a) and (b) show the XRD patterns of S4-3 alloy (with only La addition) and S4-4 alloy (with only Ce addition), respectively. In the alloy with La addition, weak peaks of Al_2La and $\text{Al}_{11}\text{La}_3$ compounds are detected (Fig. 4(a)), besides $\alpha\text{-Al}$, Si, $\text{Al}_{15}\text{Mn}_3\text{Si}_2$ and CuAl_2 phases. In the alloy with Ce addition, Ce-rich compounds of AlCe_3 , Al_4Ce , $\text{Al}_{10}\text{Cu}_7\text{Ce}_2$ and $\text{Al}_{92}\text{Ce}_8$ are also detected though the peak intensities of them are weak (Fig. 4(b)). This indicates that La-rich and/or Ce-rich compounds are formed with addition of La and/or Ce into aluminum melts. Besides the above La- and Ce-aluminides, by careful comparison with PDF

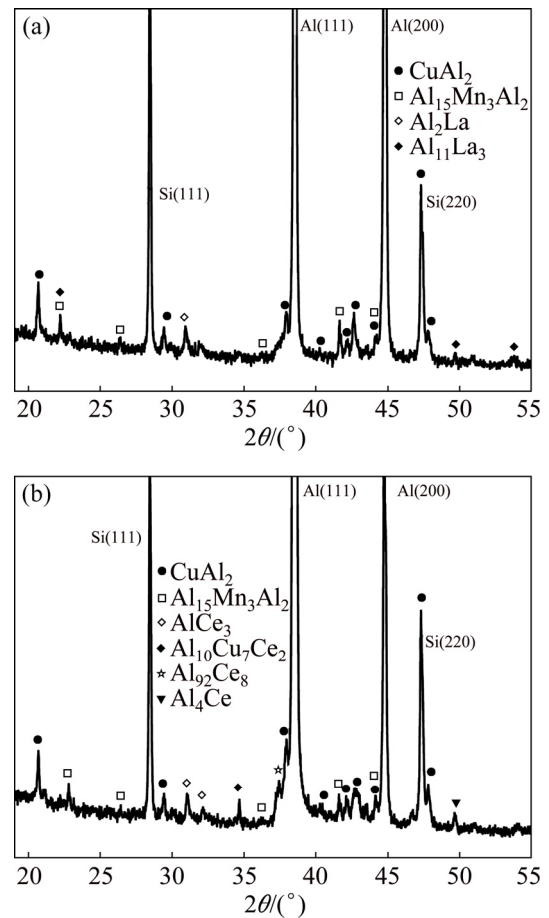


Fig. 4 XRD results of as-cast S4-3 (a) and S4-4 (b) alloys

cards database, no other potential compounds (such as Al-Si-RE, Al-Cu-RE or Al-Si-Cu-RE compounds) can well match these peaks even though EDS results illustrate that these needles contain high level of Si. Due to much strong affinity of La and Ce with Al, La- and Ce-aluminides can form at early stage of solidification, usually prior to the formation of most compounds in a great variety of aluminum alloys. By combination of EDS results and morphology observation of these needles and XRD analysis of the studied alloys, La- and Ce-aluminides are thought to be firstly formed at the early stage of solidification, growing in the form of faceted crystal characteristic (fine and long needle-like). Then, during the final eutectic reaction, CuAl_2 grows on the surface of La- and Ce-aluminides as a film enveloping them.

Figure 5 shows the network-like or mass-flocculent CuAl_2 phase in S4 alloy and its EDS results. In Al-12%Si-4%Cu-1.6%Mn alloy, CuAl_2 phase is formed during the final eutectic reaction at 522 °C: $L \rightarrow \alpha\text{-Al} + \text{Si} + \text{Al}_{15}\text{Mn}_3\text{Si}_2 + \text{CuAl}_2$ (by PandatTM). It occurs at the end of solidification, thus most of CuAl_2 phase segregates as network-like or mass-flocculent phase at the eutectic grain boundaries. However, RE addition, whether mish metal, La or Ce, completely alters its

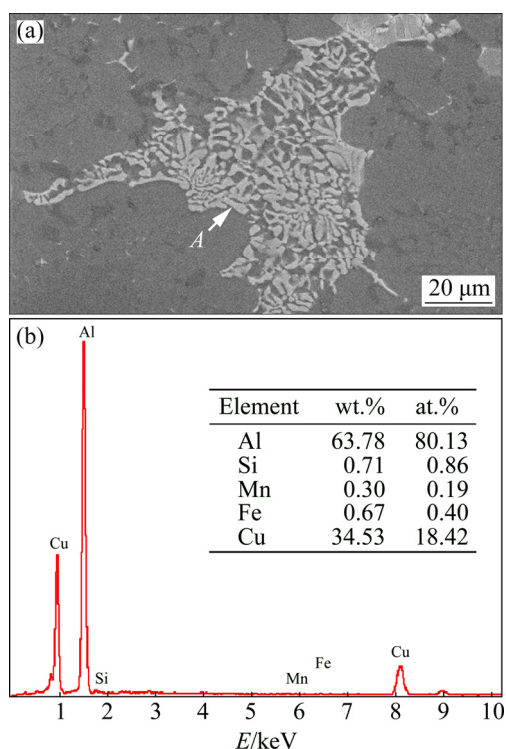


Fig. 5 Morphology of CuAl_2 phase in S4 alloy (a) and its EDS results (b)

morphology, as shown in Fig. 6, and also in Fig. 2. Most of CuAl_2 phase becomes discretely blocky, entangled with hair-filamentous RE-rich needles and blocky Si particulates. Figure 7 shows entangled CuAl_2 and RE-rich phases in S4-3 alloy. The fine needles marked by zone A in Fig. 7(a) are RE-rich (by EDS in Fig. 7(b)). The bright blocky B and C are demonstrated as CuAl_2 by EDS detection (Figs. 7(c) and (d), respectively). This

suggests that the CuAl_2 phase grows on the RE-rich needles. And it is also seen that there are a great number of small bright germs of CuAl_2 phases on the fine needles (as seen in Figs. 6 and Fig. 7(a)). This indicates that the formation of CuAl_2 phase is closely tied with RE-rich needles.

In S4-2 alloy with addition of mish metal (in which La and Ce are the main constituents), an interesting phenomenon is revealed in Fig. 8. CuAl_2 block (zone C), $\text{Al}_{15}\text{Mn}_3\text{Si}_2$ particulate (zone B) and RE-rich needle (zone A) co-grow, and CuAl_2 and $\text{Al}_{15}\text{Mn}_3\text{Si}_2$ phases grow on the RE-rich needles. In another alloy with only Ce addition (S4-4), the same phenomenon occurs, as seen in Fig. 9. However, in the alloy with only La addition (S4-3), this phenomenon does not occur. This indicates that Ce existence in S4-2 and S4-4 alloys plays a key role in the co-growth of $\text{Al}_{15}\text{Mn}_3\text{Si}_2$ phase with the needle-like RE-rich phase. From the above observation, it is concluded that RE addition completely alters the solidification process of CuAl_2 phase, from network-like or mass-flocculent phase (without RE addition) in the form of segregation at the final eutectic grain boundaries into discretely blocky phase that grows on the hair-filamentous RE-rich needles. And the eutectic $\text{Al}_{15}\text{Mn}_3\text{Si}_2$ phase grows in the same way in the alloys with Ce existence.

La- and Ce-aluminides can form at the early stage of solidification, usually prior to the formation of most compounds in a great variety of aluminum alloys. From Al-rich corner of Al-La and Al-Ce binary phase diagrams, the temperature to form La- and Ce-aluminides is usually above 600 °C. By Pandat™ software, the eutectic reaction of $L \rightarrow \alpha\text{-Al} + \text{Si} +$

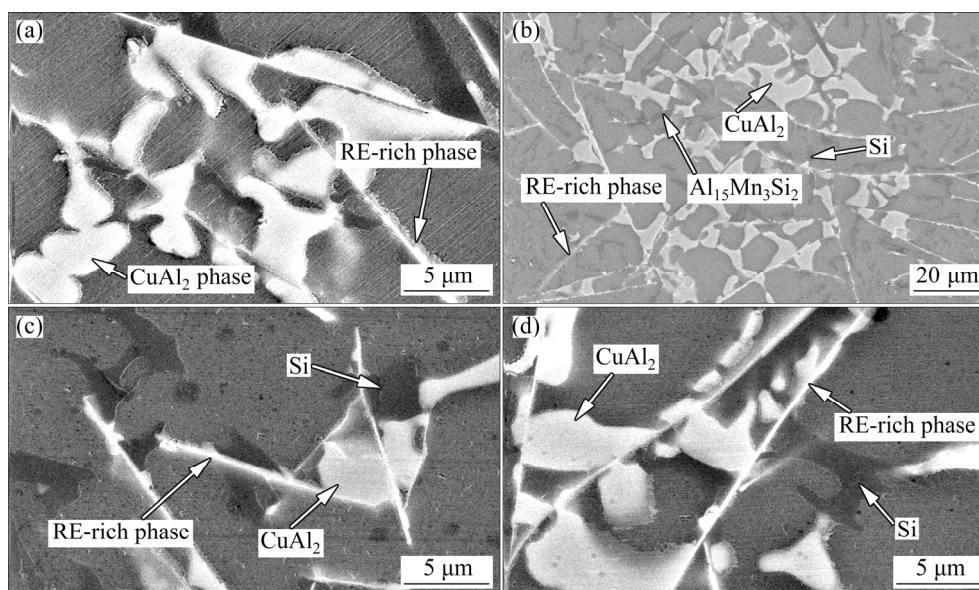


Fig. 6 Discrete blocky CuAl_2 phase growing on hair-filamentous RE-rich needles in different alloys with RE addition: (a) S4-1 alloy; (b) S4-2 alloy; (c) S4-3 alloy; (d) S4-4 alloy

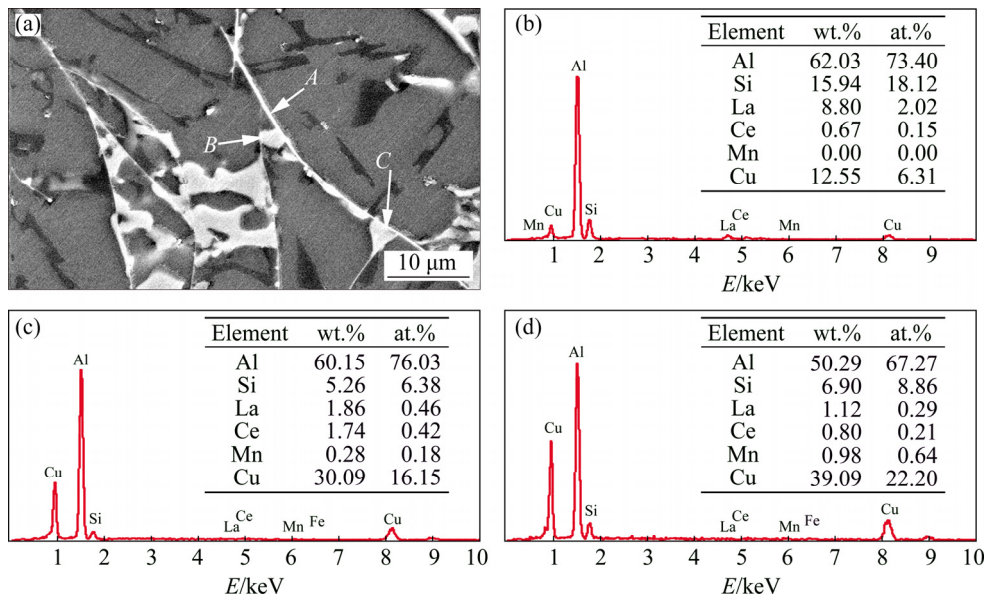


Fig. 7 Entangled CuAl_2 and RE-rich phases in S4-3 alloy (a) and EDS results (b–d corresponding to zones A, B and C in (a), respectively)

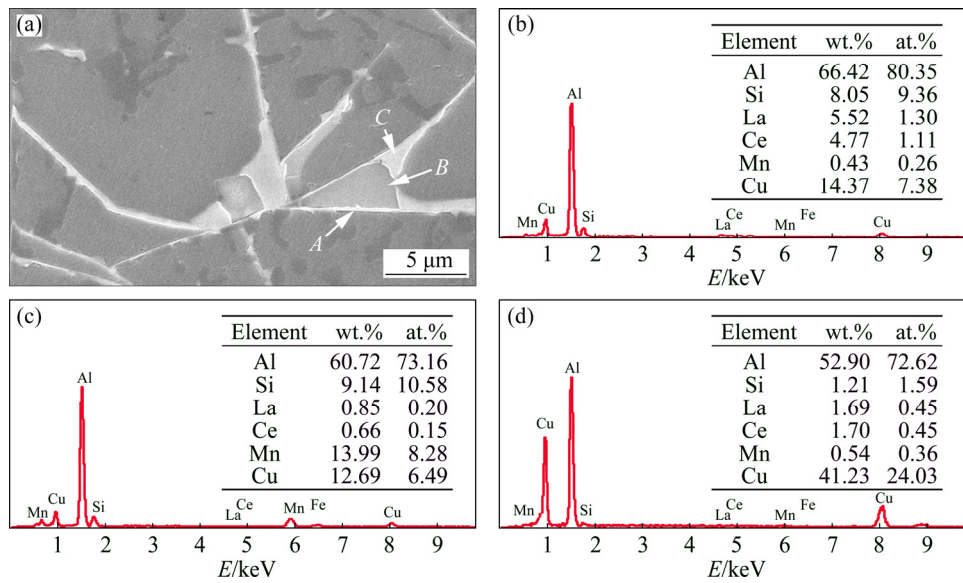


Fig. 8 Co-growth relations of CuAl_2 , $\text{Al}_{15}\text{Mn}_3\text{Si}_2$ and RE-rich phases in S4-2 alloy (a) and EDS results (b–d corresponding to zones A, B and C in (a), respectively)

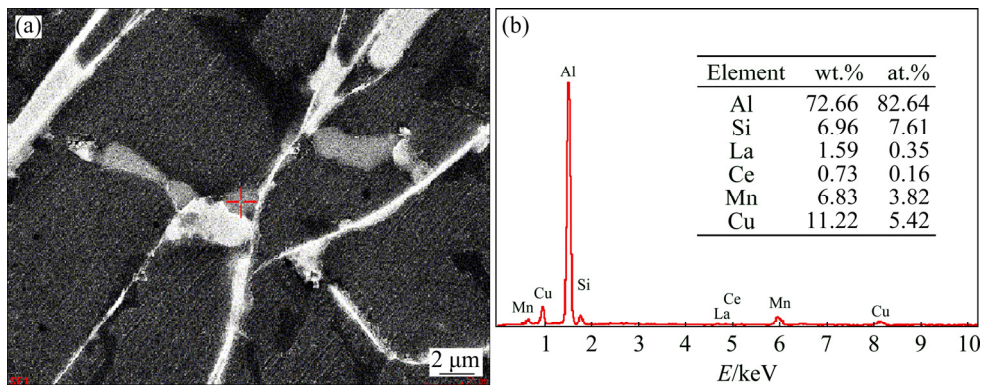


Fig. 9 Co-growth relations of CuAl_2 , $\text{Al}_{15}\text{Mn}_3\text{Si}_2$ and RE-rich phases in S4-4 alloy (a) and EDS results of light grey $\text{Al}_{15}\text{Mn}_3\text{Si}_2$ particle (b)

$\text{Al}_{15}\text{Mn}_3\text{Si}_2+\text{CuAl}_2$ occurs at 522 °C. From Fig. 4(a), $\text{Al}_{11}\text{La}_3$ phase is detected in the alloys with La addition. Both $\text{Al}_{11}\text{La}_3$ and CuAl_2 belong to tetragonal system, of which the lattice mismatch degrees on (001) and (100) are only 7.7% and 6.2%, respectively. This indicates that $\text{Al}_{11}\text{La}_3$ has good coherent relationship with CuAl_2 phase. Needle-like $\text{Al}_{11}\text{La}_3$ phase grows in the form of typical faceted crystal. (001) or (100) is the lowest free energy plane of tetragonal crystals. For faceted-growth, the liquid/solid interfaces always consist of low energy planes, so (001) or (100) may be the exposed surface of the growing $\text{Al}_{11}\text{La}_3$ crystal. According to lattice matching mechanism, the low energy planes between two crystals are the most potential interfaces of them. As seen in Figs. 3, 6 and 7, CuAl_2 phase presents as thin film, small germ and discrete block that are closely tied with needle-like La- and Ce-aluminides. During the earliest growing stage of CuAl_2 phase, it grows by lateral step mechanism. (001) or (100) of CuAl_2 phase may grow on the surface of $\text{Al}_{11}\text{La}_3$, and hence it is in the form of film shape. Therefore, it is deduced that $\text{Al}_{11}\text{La}_3$ crystal that is formed prior to CuAl_2 can act as the heterogeneous nucleation sites for the latter. The addition of La could alter the nucleation and growth of CuAl_2 phase during the final eutectic reaction. CuAl_2 crystal preferentially forms with a shape of thin film firstly on the surface of $\text{Al}_{11}\text{La}_3$ needles, and then protrudes locally in the form of small germs, and finally grows freely in the liquid into blocky phase. As a result, the morphology of CuAl_2 phase changes from network-like or mass-flocculent into discrete blocky phase. Due to the addition of Ce, the prior formed Al_4Ce phase also has good coherent relationship with CuAl_2 phase, and therefore the

addition of Ce also produces a similar impact to the crystallization process of CuAl_2 phase.

The start crystallizing temperature of primary $\text{Al}_{15}\text{Mn}_3\text{Si}_2$ phase in Al–12%Si–4%Cu–1.6%Mn alloy is 633 °C by Pandat™ software. The temperature to form potential RE-rich compounds may be below this temperature. Therefore, the addition of RE has no influence on the formation of the primary $\text{Al}_{15}\text{Mn}_3\text{Si}_2$ phase. For eutectic $\text{Al}_{15}\text{Mn}_3\text{Si}_2$ phase, it is mainly from two eutectic reactions, the main eutectic reaction of $L \rightarrow \alpha\text{-Al}+\text{Si}+\text{Al}_{15}\text{Mn}_3\text{Si}_2$ (in a temperature range of 569–522 °C) and the last eutectic reaction described above (at a constant temperature of 522 °C). $\text{Al}_{15}\text{Mn}_3\text{Si}_2$ formed in Al–Si–Cu–Mn alloy has been demonstrated to have body-centered cubic structure [20]. In the alloy with Ce addition, Al_9Ce_8 crystal is detected (Fig. 4(b)). This Ce-aluminide has the same body-centered cubic structure as $\text{Al}_{15}\text{Mn}_3\text{Si}_2$, and the lattice mismatch degree between them is only 0.4%. So, this Ce-aluminide has a very high coherent relationship with $\text{Al}_{15}\text{Mn}_3\text{Si}_2$, thus has powerful ability as heterogeneous nucleation sites for eutectic $\text{Al}_{15}\text{Mn}_3\text{Si}_2$. This is the reason for that CuAl_2 block, $\text{Al}_{15}\text{Mn}_3\text{Si}_2$ particulate and RE-rich needle co-grow in the alloys with Ce addition (Figs. 8 and 9). However, even $\text{Al}_{11}\text{La}_3$ crystal is formed prior to eutectic $\text{Al}_{15}\text{Mn}_3\text{Si}_2$ compound, the lattice mismatch degree between them is too large to act as nucleation sites for eutectic $\text{Al}_{15}\text{Mn}_3\text{Si}_2$, so, in the alloy with only La addition (S4-3), the co-growing phenomenon does not occur. It is rational to think that Ce addition could alter the crystallizing course of eutectic $\text{Al}_{15}\text{Mn}_3\text{Si}_2$, but La addition could not.

Figure 10 shows the microstructures of the studied

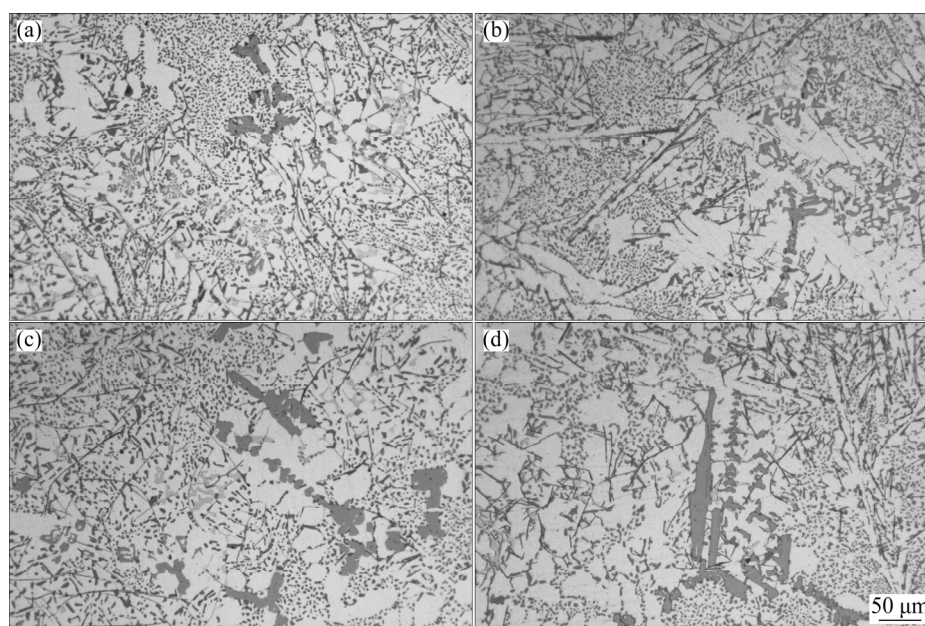


Fig. 10 Optical microscopic images showing microstructures of studied alloys after solutionizing at 510 °C for 5 h: (a) S4-1 alloy; (b) S4-2 alloy; (c) S4-3 alloy; (d) S4-4 alloy

alloys after solutionizing at 510 °C for 5 h. This thermal history does not alter the morphology and size of primary $\text{Al}_{15}\text{Mn}_3\text{Si}_2$ phase, consistent with the result in Ref. [14]. In Fig. 10, a great number of fine RE-rich needles are still observed, illustrating that these RE-rich needles formed during solidification also have excellent thermal stability.

3.2 Tensile strength at high temperature

It was reported that the complex RE-rich compounds formed in Al–Si alloy with RE addition could improve the high-temperature strength [7,17]. But, in our study, the formed RE-rich phases present as fine needle, which has strong cutting effect during tension, and thus they may deteriorate the strength. Table 2 lists the tensile strength of the studied alloys at 200 and 300 °C after T6 treatment (solutionizing at 510 °C for 5 h and aging at 165 °C for 6 h). The addition of small amount of RE (0.5 wt.% addition level, in S4-1, S4-3 and S4-4), whether MM, sole La or sole Ce, only results in a slight increase in strength at both 200 and 300 °C. When the addition level is further increased (in S4-2), the strength is conversely decreased slightly. Even the new formed RE-rich compounds have good thermal stability, the addition of RE does not exhibit the expected improvement in strength at high temperature. This may be due to the strong cutting effect from its fine needle-like morphology.

Table 2 Tensile strength of studied alloys at 200 and 300 °C

Alloy	Ultimate tensile strength (T6 temper)/MPa	
	200 °C	300 °C
S4	207.4	119.3
S4-1	211.9	125.3
S4-2	196.7	120.7
S4-3	218.2	128.2
S4-4	214.9	125.2

Figure 11(a) shows the fractograph of S4-1 alloy (T6) after tensile test at 300 °C. There are a number of tearing ridges, a great amount of cleavage planes and a lot of cracks, illustrating that it is a brittle rupture. The EDS on cleavage plane (Fig. 11(b)) suggests that the fracture occurs throughout the primary $\text{Al}_{15}\text{Mn}_3\text{Si}_2$ dendrites. No RE-rich needles appear on the fracture surface. Figure 12 also reveals that micro-cracks interiorly originate in the primary $\text{Al}_{15}\text{Mn}_3\text{Si}_2$ phase, but not the needle-like RE-rich phase. The frangibility of the primary $\text{Al}_{15}\text{Mn}_3\text{Si}_2$ phase is dominant in originating and propagating of micro-cracks during tensile test. This indicates that even the fine RE-rich needles have strong cutting effect (prone to stress-concentrating), the addition

of RE into Al–12%Si–4%Cu–1.6%Mn does not significantly alter the micro-crack's originating and propagating and fracture characteristics.

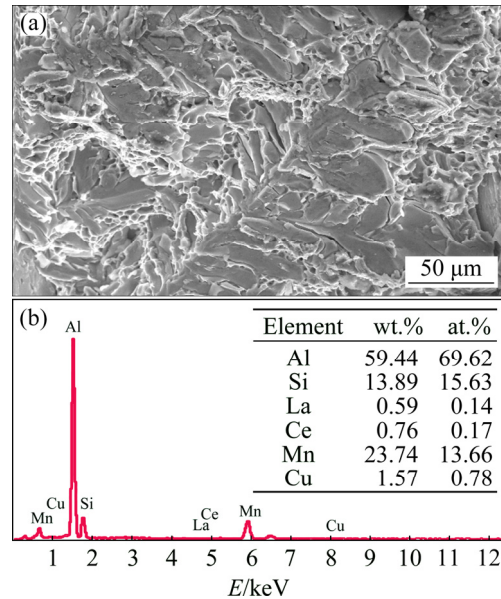


Fig. 11 SEM image showing fractograph of S4-1 alloy (T6) after tensile test at 300 °C (a) and EDS results on cleavage plane (b)

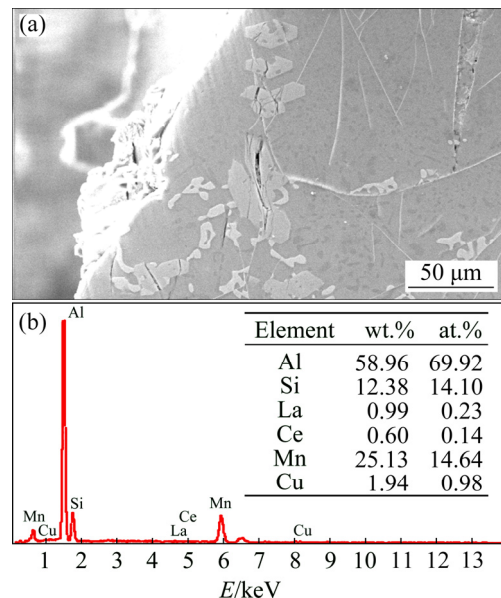


Fig. 12 SEM image showing microstructure near fracture surface of S4-1 alloy (T6) after tensile test at 300 °C (a) and EDS results of zone with small cracks

4 Conclusions

(1) RE addition does not refine the primary Mn-rich phase as expected. However, it completely alters the morphology of CuAl_2 phase into discrete and blocky phase, which is due to the prior formed La- and

Ce-aluminides that could act as the heterogeneous nucleation site for CuAl_2 phase.

(2) In the alloys with Ce addition, an interesting phenomenon occurs that CuAl_2 block, $\text{Al}_{15}\text{Mn}_3\text{Si}_2$ particulate and RE-rich needle are co-growing, but this does not occur in the alloy with only La addition. Al_2Ce_8 has a very high coherent relationship with $\text{Al}_{15}\text{Mn}_3\text{Si}_2$ phase, so the addition of Ce alters the crystallizing course of eutectic $\text{Al}_{15}\text{Mn}_3\text{Si}_2$ phase.

(3) These fine needle-like La- and Ce-aluminides have good thermal stability even under a thermal history of 510 °C for 5 h. However, the addition of small amount of RE (0.5 wt.% addition level), whether MM, sole La or sole Ce, only results in a slight increase in strength at both 200 and 300 °C. But when addition level is further increased, the strength is conversely decreased slightly.

(4) Even these fine RE-rich needles have strong cutting effect, the addition of RE into Al–12%Si–4%Cu–1.6%Mn alloy does not significantly alter the originating and propagating of micro-cracks and fracture characteristics during tensile deformation.

References

- [1] KARAMOUZ M, AZARBARMAS M, EMAMY M. On the conjoint influence of heat treatment and lithium content on microstructure and mechanical properties of A380 aluminum alloy [J]. *Materials & Design*, 2014, 59: 377–382.
- [2] IRIZALP S G, SAKLAKOGLU N. Effect of Fe-rich intermetallics on the microstructure and mechanical properties of thixo-formed A380 aluminum alloy [J]. *Engineering Science and Technology*, 2014, 17(2): 58–62.
- [3] KARAMOUZ M, AZARBARMAS M, EMAMY M, ALIPOUR M. Microstructure, hardness and tensile properties of A380 aluminum alloy with and without Li additions [J]. *Materials Science and Engineering A*, 2013, 582: 409–414.
- [4] YANG Yang, LI Yun-guo, LIU Xiang-fa. Evolution of the rich-nickel intermetallics of high-iron Al–Si piston alloy [J]. *Transactions of Materials and Heat Treatment*, 2011, 32(S): s86–s89. (in Chinese)
- [5] WANG Jin-guo, ZHOU Hong, KEISAKU O, KANG H G. Influence of Ni and Mn on solidification microstructure and ageing hardening of Al–Si–Cu–Mg alloys [J]. *The Chinese Journal of Nonferrous Metals*, 2000, 10(S1): s168–s172. (in Chinese)
- [6] LI Run-xia, LI Rong-de, LÜ Wei, QU Ying-dong, LI Chen-xi. Effects of solution heat treatment on microstructures and properties of Al–Si–Cu–Mg cast alloys [J]. *The Chinese Journal of Nonferrous Metals*, 2007, 17(2): 193–199. (in Chinese)
- [7] ZHANG Wen-da, YANG Jing, LIU Yun, DANG Jin-zhi, XU Hong. Effect of Y on high temperature mechanical properties of AlSi7Cu2Mg alloy [J]. *The Chinese Journal of Nonferrous Metals*, 2013, 23(7): 1855–1860. (in Chinese)
- [8] FENG Z Q, YANG Y Q, HUANG B, LI M H, CHEN Y X, RU J G. Crystal substructures of the rotation-twinned T ($\text{Al}_{20}\text{Cu}_2\text{Mn}_3$) phase in 2024 aluminum alloy [J]. *Journal of Alloys and Compounds*, 2014, 583: 445–451.
- [9] CHEN Z, CHEN P, LI S. Effect of Ce addition on microstructure of $\text{Al}_{20}\text{Cu}_2\text{Mn}_3$ twin phase in an Al–Cu–Mn casting alloy [J]. *Materials Science and Engineering A*, 2012, 532: 606–609.
- [10] MOHANED A M, SAMUEL A M, SAMUEL F H, DOTY H W. Influence of additives on the microstructure and tensile properties of near-eutectic Al–10.8%Si cast alloy [J]. *Materials & Design*, 2009, 30(10): 3943–3957.
- [11] LIU K, CAO X, CHEN X G. Effect of Mn, Si, and cooling rate on the formation of iron-rich intermetallics in 206 Al–Cu cast alloys [J]. *Metallurgical and Materials Transactions B*, 2012, 43(5): 1231–1240.
- [12] CESCHINI L, BOROMEI I, MORRI A, SEIFEDDINE S, SVENSSON I L. Microstructure, tensile and fatigue properties of the Al–10%Si–2%Cu alloy with different Fe and Mn content cast under controlled conditions [J]. *Journal of Materials Processing Technology*, 2009, 209(15–16): 5669–5679.
- [13] LIAO H C, TANG Y Y, SUO X J, LI G J, HU Y Y, DIXIT S U, PETROV P. Dispersoid particles precipitated during the solutionizing course of Al–12wt.%Si–4wt.%Cu–1.2wt.%Mn alloy and their influence on high temperature strength [J]. *Materials Science and Engineering A*, 2017, 699: 201–209.
- [14] LI G J, LIAO H C, SUO X J, TANG Y Y, DIXIT S U, PETROV P. Cr-induced morphology change of primary Mn-rich phase in Al–Si–Cu–Mn heat resistant aluminum alloys and its contribution to high temperature strength [J]. *Materials Science and Engineering A*, 2018, 709: 90–96.
- [15] CHANG J, MOON I, CHOI C. Refinement of cast microstructure of hypereutectic Al–Si alloys through the addition of rare earth metals [J]. *Journal of Materials Science*, 1998, 33(20): 5015–5023.
- [16] KAUR P, DWIVEDI D K, PATHAK P M. Effects of electromagnetic stirring and rare earth compounds on the microstructure and mechanical properties of hypereutectic Al–Si alloys [J]. *The International Journal of Advanced Manufacturing Technology*, 2012, 63(1–4): 415–420.
- [17] LI Pei-jie, ZENG Da-ben, JIA Jun, LI Qing-chun. Influence of La on elevated temperature property of ZL702 [J]. *Journal of the Chinese Rare Earth Society*, 2000, 18(2): 187–189. (in Chinese)
- [18] FAN C, LONG S Y, YANG H D, WANG X J, ZHANG J C. Influence of Ce and Mn addition on α -Fe morphology in recycled Al–Si alloy ingots [J]. *International Journal of Minerals, Metallurgy, and Materials*, 2013, 20(9): 890–895.
- [19] CAI Guo-sheng, LI Zhi-long, LU Hua-feng, ZHENG Zhi-wei, CHEN Rong-fa. Influences of Ce-rich mixed RE on the microstructure and properties of as cast 2A14 aluminum alloy [J]. *Foundry*, 2014, 63(12): 1263–1265. (in Chinese)
- [20] SUO X J, LIAO H C, HU Y Y. Formation of $\text{Al}_{15}\text{Mn}_3\text{Si}_2$ phase during solidification of a novel Al–12%Si–4%Cu–1%Mn heat-resistant casting alloy and its thermal stability [J]. *Journal of Materials Engineering and Performances*, 2018, 27: 2910–2920.

稀土金属 RE 添加对 Al-12%Si-4%Cu-1.6%Mn 耐热合金凝固过程和高温强度的影响

廖恒成, 许何婷, 胡以云

东南大学 材料科学与工程学院 江苏省先进金属材料高技术重点实验室, 南京 211189

摘 要: 采用显微组织观察和拉伸实验研究稀土金属(RE)添加对 Al-12%Si-4%Cu-1.6%Mn 耐热合金凝固过程和高温强度的影响。在加入 RE 的合金中观察到大量细小针状富 RE 相, 固溶处理不能改变其形态与大小, 表明其具有良好的热稳定性。RE 的加入已完全改变共晶 CuAl_2 相的凝固过程, 从偏聚在最终共晶晶粒边界上的网络状变成离散的块状, 生长在如头发丝的富 RE 细针上。在含有 Ce 的合金中, 块状 CuAl_2 、颗粒状 $\text{Al}_5\text{Mn}_3\text{Si}_2$ 和针状富 RE 相共生在一起; 然而, 在仅加入 La 的合金中, 此共生现象并未发生。RE 的加入不能显著改善合金的高温强度。而针状富 RE 相的形成也未显著改变合金拉伸过程中微裂纹的萌生与扩展。

关键词: Al-Si-Cu-Mn 耐热合金; 稀土; 凝固过程; 高温强度

(Edited by Wei-ping CHEN)